DALTON
FULL PAPER

The first oxalate-bridged one-dimensional polymer containing Mo^{V}_2 dimers with single metal–metal bonds. Syntheses and structures of $(MeNC_5H_5)_{2n}[Mo_2O_4(C_2O_4)Cl_2]_n$ and $(3\text{-}MePyH)_{2n}[Mo_2O_4(C_2O_4)Cl_2]_n$

Barbara Modec,*[a] Jurij V. Brenčič,[a] Darko Dolenc[a] and Jon Zubieta[b]

[a] *Faculty of Chemistry and Chemical Technology, University of Ljubljana, Aškerčeva 5, 1000 Ljubljana, Slovenia. E-mail: barbara.modec@uni-lj.si*
[b] *Department of Chemistry, Syracuse University, New York 13244, USA. E-mail: jazubiet@syr.edu*

Received 1st August 2002, Accepted 18th October 2002
First published as an Advance Article on the web 18th November 2002

Hydrothermal reactions of mononuclear oxochloromolybdate(V) with oxalic acid in alcohol (methanol or 2-propanol) and pyridines (pyridine or 3-methylpyridine) media have afforded two polymeric compounds of molybdenum(V): *N*-methylpyridinum *catena*-μ-oxalato-$O^1,O^2:O^{1'},O^{2'}$-(dichloro-di-μ-oxo-dioxodimolybdate(V)), $(MeNC_5H_5)_{2n}[Mo_2O_4(C_2O_4)Cl_2]_n$ **1** and 3-methylpyridinium *catena*-μ-oxalato-$O^1,O^2:O^{1'},O^{2'}$-(dichloro-di-μ-oxo-dioxodimolybdate(V)), $(3\text{-}MePyH)_{2n}[Mo_2O_4(C_2O_4)Cl_2]_n$ **2**. The compounds were fully characterized by X-ray structural analysis, infrared and NMR spectroscopy. The essentially isostructural anionic chains in **1**and **2** are built of alternating pairs of $\{Mo_2O_4\}^{2+}$ containing edge-sharing octahedra and planar oxalates giving a Mo : oxalate ratio of 2. The bisbidentate oxalate acts as a bridge between two dinuclear subunits. The formation of a *N*-methylpyridinium cation from methanol and pyridine in the presence of molybdenum(V) and oxalic acid has not been documented before.

Introduction

Rational construction of specific architectures from molecular building blocks has been an area of active research over the past few years.[1] Examples in the oxomolybdenum(VI) chemistry range from clusters of nanosize dimensions[2] to a class of organic–inorganic composite materials with extended structures.[3] The introduced organodiamine component in the latter group either serves as a ligand to the molybdenum oxide array[4] or becomes engaged in its protonated form in hydrogen bonding interactions with the terminal and the bridging oxo groups of the molybdenum oxide skeleton.[5] The recent literature reports that discrete Keggin type anions can also be linked into polymeric materials.[6] The intense interest in these materials is driven to a large extent by their rich structural chemistry and remarkable magnetic and catalytic properties.[7]

While the polymeric oxomolybdenum(VI) compounds represent a well-developed class of materials, there is a relative paucity of data on those containing molybdenum in +5 oxidation state with polymeric structures. A dinuclear $\{Mo_2O_2(\mu\text{-}O)_2\}^{2+}$ moiety (Scheme 1), hereafter designated in short as $\{Mo_2O_4\}^{2+}$, with a single metal–metal bond between the two metal centres, presents itself as an ideal molecular building block in molybdenum(V) chemistry.

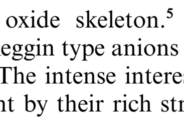

Scheme 1 A basic $\{Mo_2O_4\}^{2+}$ unit.

Not only does it dominate the chemistry of this oxidation state, but its structural integrity remains intact irrespective of the rest of the metal's environment.[8] It has a set number of bonding sites: three per metal centre with the one positioned *trans* to the molybdenyl group usually experiencing a strong *trans* influence from the multiply bonded terminal oxygen. Furthermore, the ease with which larger aggregates are formed is well-known and is also exemplified by a series of products of the polymerization reactions of mononuclear oxohalomolybdates(V) in alcohols and pyridines.[9] This seemingly simple reaction system was shown to produce several discrete clusters of different nuclearities: two, three, four or at most six $\{Mo_2O_4\}^{2+}$ units were assembled through μ-, μ_3- and μ_4-bridging oxo groups. The ready formation of larger aggregates stems from molybdenum's affinity for oxygen donor ligands combined with the ability of these to participate in bridging interactions. It seems feasible that the introduction of a multidentate ligand would lead to the linkage of dinuclear $\{Mo_2O_4\}^{2+}$ units or their larger aggregates into extended arrays. This approach has been realized to date, as will be shown presently, only with the hydrothermally prepared phosphomolybdates(V).[10] Following this analogy, we have chosen the oxalate ligand to serve the same purpose. This paper presents two compounds, $(MeNC_5H_5)_{2n}[Mo_2O_4(C_2O_4)Cl_2]_n$ **1** and $(3\text{-}MePyH)_{2n}[Mo_2O_4(C_2O_4)Cl_2]_n$ **2**, where our attempts were met with success. Both contain anionic chains made of $\{Mo_2O_4\}^{2+}$ units linked by bisbidentate oxalates. Apart from the fact that the pair represents only the second example of an extended structural type built of covalently linked $\{Mo_2O_4\}^{2+}$ units, the importance of the present work also lies in the *in situ* formation of the *N*-methylpyridinium cations which finds no precedence in the exhaustive oxomolybdenum(V) chemistry.

Experimental

Reactions were carried out in sealed glass tubes under autogenous pressure. Reagents were purchased from Aldrich and used without further purification. $(PyH)_2[MoOCl_5]$ was prepared by minor modification of a published procedure.[11] The IR and far IR spectra were measured on solid samples as Nujol or poly(chlorotrifluoroethylene) mulls using a Perkin-Elmer 2000 series FT-IR spectrometer. ^1H spectra were recorded on a Bruker Avance DPX 300 spectrometer (^1H, 300 MHz) referenced to the solvent. Elemental analyses were performed by the Chemistry Department service at the University of Ljubljana.

Synthesis of $(Me–NC_5H_5)_{2n}[Mo_2O_4(C_2O_4)Cl_2]_n$ 1

A mixture of $(PyH)_2[MoOCl_5]$ (50 mg, 0.111 mmol), $H_2C_2O_4 \cdot 2H_2O$ (10 mg, 0.0794 mmol), $(C_6H_5)_4PBr$ (19 mg, 0.0454 mmol), pyridine (4 cm^3), methanol (0.5 cm^3) and acetonitrile (0.5 cm^3) was placed in a glass tube which was sealed and subsequently heated for 120 hours in an electric oven maintained at 130 °C. After cooling to room temperature, orange crystals of compound **1** were isolated in 68% yield (24 mg). Calc. for $C_{14}H_{16}Cl_2Mo_2N_2O_8$: C, 27.88; H, 2.67; N, 4.65. Found: C, 27.68; H, 2.52; N, 4.76%. IR (cm^{-1}): 3121w, 3086w, 3065w, 3053w, 1949w, 1670vvs, 1621vvs, 1485vvs, 1417m, 1353m, 1306m, 1288m, 1211w, 1187vs, 1157m, 1131w, 1055m, 1027w, 965vvs, 943vs, 882m, 803vvs, 774vvs, 738vvs, 683vvs, 606w, 533w, 493vs, 473vs, 451s, 401s, 348w, 316vs, 286w, 269w and 235w. ^{1}H NMR (D_2O, 300 MHz), δ (ppm): 4.38 (3H, s, CH_3–NC_5H_5), 8.03 (m, 2H, H_3), 8.52 (1H, t, $J = 7.9$ Hz, H_4) and 8.77 (2H, d, $J = 6.0$ Hz, H_2).

Synthesis of $(3\text{-}MePyH)_{2n}[Mo_2O_4(C_2O_4)Cl_2]_n$ 2

A mixture of $(PyH)_2[MoOCl_5]$ (50 mg, 0.111 mmol), $H_2C_2O_4 \cdot 2H_2O$ (20 mg, 0.159 mmol), 3-methylpyridine (3 cm^3), 2-propanol (0.5 cm^3) and acetonitrile (0.5 cm^3) was placed in a glass tube which was sealed and subsequently heated for 100 hours in an electric oven maintained at 130 °C. After cooling to room temperature, orange crystals of compound **2** were isolated in 71% yield (25 mg). Calc. for $C_{14}H_{16}Cl_2Mo_2N_2O_8$: C, 27.88; H, 2.67; N, 4.65. Found: C, 27.66; H, 2.54; N, 4.48%. IR (cm^{-1}): 3227w, 3175w, 3121w, 3091w, 3066w, 3055m, 1946w, 1672vvs, 1629vvs, 1557vs, 1353vs, 1302w, 1263m, 1234w, 1185w, 1168w, 1154w, 1120m, 1083w, 1043m, 1031w, 1018w, 992w, 973vvs, 955vs, 905m, 799vvs, 724vvs, 682vvs, 626m, 547w, 534w, 501vs, 473m, 462vs, 407m, 350w, 322vs, 287w, 277m, 257w and 243w. ^{1}H NMR (D_2O, 300 MHz), δ (ppm): 2.54 (3H, s, 3-CH_3Py), 7.95 (1H, dd, $J = 6$ Hz, 8 Hz, H_5), 8.45 (1H, d, $J = 8$ Hz, H_4), 8.58 (1H, d, $J = 6$ Hz, H_6) and 8.61 (1H, s, H_2).

Crystallography

The crystals used were mounted on the tip of a glass fibre with a small amount of silicon grease and transferred to a goniometer head. Data for **1** were collected on a Bruker SMART-CCD diffractometer using graphite monochromated Mo-Kα radiation. Data processing was accomplished with the SAINT program.[12] The data were corrected for the absorption using SADABS.[13] Data for compound **2** were collected on a Nonius Kappa CCD diffractometer. Data reduction and integration were performed with the software package DENZO-SMN.[14] A specific absorption correction was not applied since the crystal was nearly equidimensional and averaging of the symmetry-equivalent reflections largely compensated for any absorption effects. For both compounds, the coordinates of some or all of the non-hydrogen atoms were found *via* direct methods using the structure solution program SHELXS.[15] The positions of the remaining non-hydrogen atoms were located by use of a combination of least-squares refinement and difference Fourier maps in the SHELXL 97 program.[15] All atoms except hydrogen atoms were refined anisotropically. The hydrogen atoms were included in the structure factor calculations at idealized positions. Figures depicting the structures were prepared by SHELXTL.[16] Cell parameters and refinement results for both compounds are summarized in Table 1. Selected bond distances and angles are given in Table 2.

CCDC reference numbers 191083 and 191084.

See http://www.rsc.org/suppdata/dt/b2/b207544j/ for crystallographic data in CIF or other electronic format.

Table 1 Crystallographic data for **1** and **2**

	1	2
Empirical formula	$C_{14}H_{16}Cl_2Mo_2N_2O_8$	$C_{14}H_{16}Cl_2Mo_2N_2O_8$
Formula weight	603.07	603.07
Crystal system	Monoclinic	Monoclinic
Space group	*C*2/*c*	*C*2/*c*
T/K	150(2)	150(2)
a/Å	20.068(3)	19.1863(2)
b/Å	8.8105(12)	9.4007(2)
c/Å	12.466(2)	12.6223(2)
β/°	120.073(5)	122.9510(8)
V/Å^3	1907.4(5)	1910.39(5)
Z	4	4
λ/Å	0.71073	0.71073
μ/mm^{-1}	1.641	1.641
Collected reflections	6166	4171
Unique reflections, R_{int}	2296, 0.0391	2185, 0.0134
Observed reflections	1926	2030
$R1$ [$I > 2\sigma(I)$]	0.0314	0.0208
$wR2$ (all data)	0.0808	0.0558

Table 2 Selected bond lengths (Å) and angles (°) for **1** and **2**[a]

	1	2
Mo–Mo[b]	2.5607(7)	2.5832(4)
Mo–O(1)	1.680(2)	1.6767(16)
Mo–O(2)	1.918(2)	1.9305(15)
Mo–O(2)[b]	1.942(2)	1.9600(16)
Mo–O(3)	2.312(2)	2.3183(16)
Mo–O(4)	2.172(2)	2.1684(15)
Mo–Cl	2.4666(8)	2.4432(6)
O(1)–Mo–O(3)	161.80(9)	161.15(7)
O(1)–Mo–O(2)	108.84(10)	108.93(7)
O(1)–Mo–O(2)[b]	105.74(10)	106.55(7)
O(1)–Mo–O(4)	90.45(9)	90.14(7)
O(1)–Mo–Cl	94.42(8)	94.71(6)
O(3)–Mo–O(2)[b]	80.37(8)	80.15(6)
O(3)–Mo–O(4)	72.65(7)	72.44(6)
O(3)–Mo–Cl	77.94(6)	77.69(4)
O(3)–Mo–O(2)	87.55(8)	87.94(6)
O(2)[b]–Mo–O(4)	86.16(9)	86.59(6)
O(4)–Mo–Cl	85.51(6)	87.16(4)
Cl–Mo–O(2)	87.76(7)	85.98(5)
O(2)–Mo–O(2)[b]	93.31(10)	92.84(7)
Mo–O(2)–Mo[b]	83.10(9)	83.20(6)

[a] The same labelling scheme pertains to the chains in **1** and **2**. [b] Related through symmetry: $1 - x, y, 0.5 - z$.

Results and discussion

Crystal structures

The structures of **1** and **2** are built of polymeric anions with the $[Mo_2O_4(C_2O_4)Cl_2]_n^{2n-}$ composition and cations, *N*-methylpyridinium cations in **1** and protonated 3-methylpyridine in **2**, respectively. Fig. 1 presents the dinuclear subunit and the countercation in **1**. The polymeric chain found in **1** and **2** is shown in Fig. 2, while Fig. 3 shows the way the chains and the cations in **2** are packed together. The dinuclear $\{Mo_2O_4\}^{2+}$ building blocks are linked by the planar oxalate ligands adopting a bisbidentate binding mode: each oxalate coordinates through two oxygen atoms to the metal from one $\{Mo_2O_4\}^{2+}$ unit and with the other two oxygen atoms to the metal from the neighbouring $\{Mo_2O_4\}^{2+}$ unit. The shortest separation between two molybdenum atoms from two adjacent dinuclear blocks bridged by the oxalate is 5.8398(8) Å in **1** and 5.8545(4) Å in **2**. The highly distorted octahedral environment of each molybdenum consists of a pair of bridging oxygen atoms, a terminal oxygen atom, a chloride and an oxalate, which binds with two distinct bond distances, 2.172(2) *vs.* 2.312(2) Å in **1**, and 2.1684(15) *vs.* 2.3183(16) Å in **2**. This difference can be

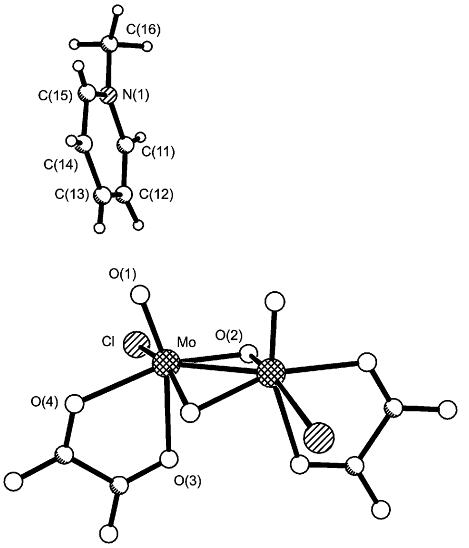

Fig. 1 A drawing of *N*-methylpyridinium cation and dinuclear subunit with the bridging oxalates in **1** showing the atom labelling scheme.

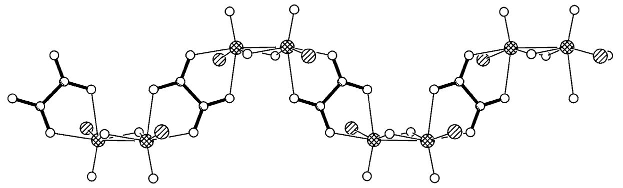

Fig. 2 A longer section of a single $[Mo_2O_4(C_2O_4)Cl_2]_n^{2n-}$ chain. Mo sites are cross-hatched; chlorides are lined bottom left to top right; oxygen atoms are unshaded and carbon atoms shaded, small sized spheres, respectively.

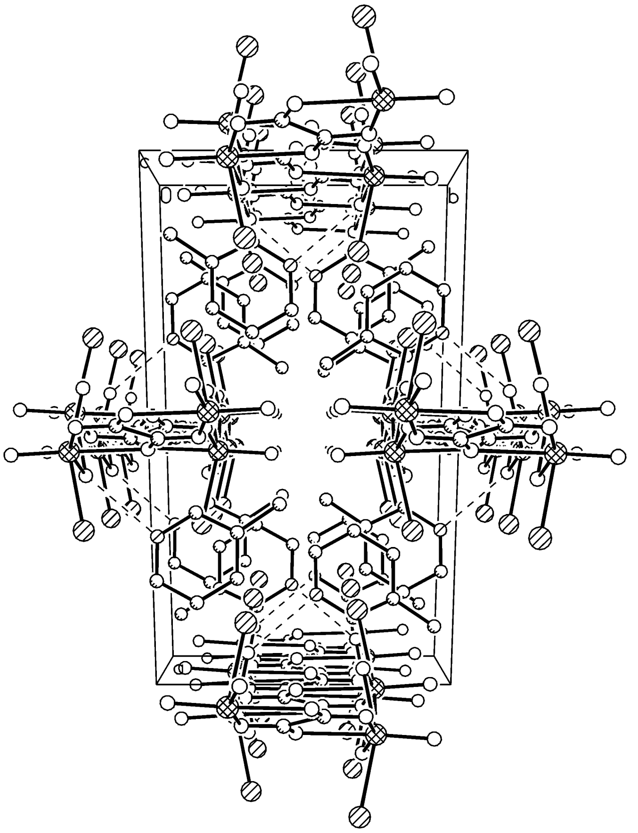

Fig. 3 Packing diagram of **2** viewed along the *c*-axis showing bundles of anionic chains which propagate perpendicular to the *ab* plane.

explained in terms of the *trans* influence of a strong, multiple bond between Mo and the terminal oxygen: O(3) occupies the position *trans* to the molybdenyl group, whilst O(4)'s position is *trans* to one of the bridging oxygens. The angles subtended at the metal by the bidentate oxalate are 72.65(7)° in **1** and 72.44(6)° in **2**. In general, the oxalate bite angles are largely determined by the metal–oxygen distances: when these are longer than 2.1 Å, the oxygen–metal–oxygen angles become smaller than 80°.[17] The bond lengths and angles of the oxalate ligand are in accord with those reported previously for other compounds in which it also acts as a bisbidentate ligand.[18]

The dinuclear building block displays a twofold rotational symmetry with the rotation axis passing through the centre of the $Mo_2(\mu\text{-}O)_2$ ring. The geometry of the $\{Mo_2O_4\}^{2+}$ unit follows the same pattern as observed in numerous $\{Mo_2O_4\}^{2+}$ containing compounds:[8] (a) folding of the $Mo_2(\mu\text{-}O)_2$ ring with the dihedral angle about the $O(2) \cdots O(2)^i$ line ((i) symmetry equivalent: $1 - x, y, 0.5 - z$) of 150.21(8)° for **1** and 148.77(6)° for **2**, (b) a short distance between metal atoms, 2.5607(7) Å for **1** and 2.5832(4) Å for **2**, which indicates a direct metal–metal bond. The structural parameters of the $\{Mo_2O_4\}^{2+}$ units in the polymeric species **1** and **2** compare well with the molecular counterparts listed in Table 3.

The chains run along the crystallographic *c*-axis. The overall conformation of the chain is sinusoidal with a period corresponding to the length of the *c* lattice constant. Since the overall shape of the cations is the same, a hexanuclear, planar ring with a methyl substituent, the cationic species, *N*-methylpyridinium cations in **1** and 3-methylpyridinium cations in **2**, occupy the same positions in the interchain regions. The cations differ only in the position of a nitrogen and one ring carbon atom (Scheme 2). However, the protonated 3-methylpyridine forms a relatively short hydrogen bond with a bridging oxygen (O2) from the anionic chain: the $N \cdots O(2)$ contact is 2.770(3) Å (Fig. 4). *N*-Methylpyridinium cation can not form hydrogen bonds of this type, thus the shortest contact between the cations and the chain in **1** is longer, 3.218(5) Å and it occurs as expected between *meta* carbon atom C(12) and O(2). The sparing solubility of both **1** and **2** in water allowed us to obtain the NMR spectra which further substantiate the nature of the cationic species (*vide supra*).

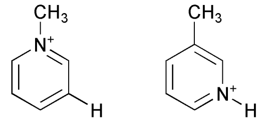

1 **2**

Scheme 2 **1** = *N*-Methylpyridinium cation; **2** = 3-methylpyridinium cation.

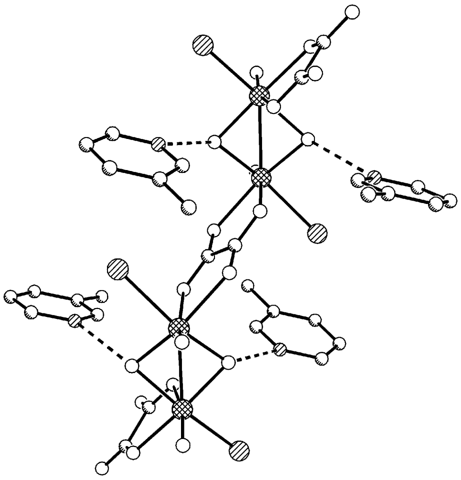

Fig. 4 Hydrogen bonds between 3-methypyridinium cations and bridging oxo groups from the anionic chain in **2**.

All of the other known $\{Mo_2O_4\}^{2+}$ complexes with oxalate are limited to discrete oligonuclear cores. The survey reveals the oxalate in two of the several possible coordination modes, none

Table 3 Comparison of some geometric parameters of $\{Mo_2O_4\}^{2+}$ units in various compounds

	Mo–Mo	Mo–O$_t$[a]	Mo–O$_b$[b]	Ref.
$Ba[Mo_2O_4(\eta^2\text{-}C_2O_4)_2(H_2O)_2]\cdot 3H_2O$[c]	2.561(1)	1.681(5)	1.930(3), 1.933(3)	19
$[Mo_2O_4Cl_2(\eta^2\text{-NP})_2]$[d]	2.5700(8)	1.678(4), 1.693(4)	1.940(5)–1.951(4)	20
$K_6[\{Mo_2O_4(\eta^2\text{-mal})_2\}_2(\mu_4\text{-mal})]\cdot 4H_2O$[e]	2.555	1.684	1.934	21
$(PyH)_2[Mo_4O_8(OMe)_2(HOMe)_2Cl_4]$	2.6005(4)	1.678(2), 1.682(2)	1.936(2)–1.990(2)[f]	9*h*
$(PyH)_2[Mo_4O_8(OEt)_2(HOEt)_2Br_4]$	2.6060(4)	1.672(2), 1.678(2)	1.934(2)–1.992(2)[f]	9*h*
$[Mo_4O_8(OMe)_2Cl_2Py_4]$	2.5966(6)	1.682(3), 1.682(4)	1.920(3)–2.007(3)[f]	9*e*
$[Mo_4O_8(OEt)_2Br_2Py_4]$	2.5795(7), 2.5872(7)	1.679(4)–1.686(5)	1.924(4)–2.008(4)[f]	9*h*
$[Mo_4Nb_2O_8(O^iPr)_{14}]$[g]	2.5837(8)	1.666(4), 1.671(4)	1.910(4)–1.930(4)	22
$(NH_4)_5[Mo_6O_{12}(CO_3)_4(OH)_3]\cdot 0.5MeOH$[h]	2.5884(6)	1.674(4)	1.948(4)	23
1	2.5607(7)	1.680(2)	1.918(2), 1.942(2)	This work
2	2.5832(4)	1.6767(16)	1.9305(15), 1.9601(16)	This work

[a] O$_t$ denotes a terminal oxygen atom. [b] O$_b$ denotes a pair of oxo bridges which span two metal atoms connected by a single metal–metal bond. [c] Redetermined values are listed. [d] NP = 2-pyridyl(diisopropylphosphino)methane. [e] mal = malonate, $CH_2(CO_2)_2^{2-}$. [f] One of the bridging oxygens is a μ_3-ligand obtained upon fusion of two $\{Mo_2O_4\}^{2+}$ units to form a tetranuclear core. [g] Two $\{Mo_2O_4\}^{2+}$ units are bridged by a pair of isopropoxo groups to form a chain whose ends are capped with secondary metals, Nb in this case. [h] A hexanuclear anion made of three $\{Mo_2O_4\}^{2+}$ units.

of these modes matches the binding mode observed in **1** and **2**. In dinuclear $[Mo_2O_4(\eta^2\text{-}C_2O_4)_2(H_2O)_2]^{2-}$ the oxalate functions as a terminal, bidentate ligand,[19,24] while in $[Mo_8O_{16}(OR)_8(C_2O_4)]^{2-}$ (R = Me, Et)[25,26] as a μ_8-ligand. The latter possesses a ring structure constructed of four dinuclear units alternately bridged by alkoxide pairs. The ring's central cavity is of perfect size to accommodate an oxalate, each of its oxygen atoms bridges a pair of molybdenum atoms from two neighbouring $\{Mo_2O_4\}^{2+}$ units. In addition to a bidentate binding mode, a quadruply bridging mode where each of the oxalate's oxygens is bound to a different metal atom was observed in the tetranuclear anions, $\{(Mo_2O_2(\mu\text{-}O)(\mu\text{-}S)(\eta^2\text{-}C_2O_4)_2)_2(\mu_4\text{-}C_2O_4)\}^{6-}$ and $\{(Mo_2O_2(\mu\text{-}S)_2(\eta^2\text{-}C_2O_4)_2)_2(\mu_4\text{-}C_2O_4)\}^{6-}$,[27,28] which are composed of $\{Mo_2O_4\}^{2+}$ analogues $\{Mo_2O_2(\mu\text{-}O)(\mu\text{-}S)\}^{2+}$ or $\{Mo_2O_2(\mu\text{-}S)_2\}^{2+}$ where one or both bridging oxygen atoms are replaced by sulfur. The aforementioned di- and octa-nuclear species share a common structural feature: the molybdenyl group lies in the same plane as the oxalate. The in-plane orientation of the terminal oxo groups accompanies oxalate in many of its binding modes,[29] also in **1** and **2** where it acts as a bisbidentate ligand. The compounds with the $[Mo_2O_4(\eta^2\text{-}C_2O_4)_2(H_2O)_2]^{2-}$ anions invoked interest because in no instance was a significant lengthening of the bonds *trans* to the terminal oxo ligands observed.[19,24] The phenomenon was ascribed to a low *trans* susceptibility of the oxalato ligand.[30] A highly asymmetrical coordination of the oxalate is evident in **1** and **2**. Since the oxalate coordination in dinuclear species and in polymeric chains in **1** and **2** is not the same, no direct comparison can be made.

Examples of extended structures built of covalently linked $\{Mo_2O_4\}^{2+}$ cores can only be found among the phosphomolybdates(v).[10] Single $\{Mo_2O_4\}^{2+}$ moieties[31] or compact assemblies of two dinuclear units,[32–34] commonly described as cube-like $\{Mo_4O_4(\mu_3\text{-}O)_4\}^{4+}$ cores, are connected by the tetrahedral phosphates into extended arrays which include one-dimensional polymers, two-dimensional layered materials and three-dimensional solids. The connectivity in the latter group is usually described in terms of alternating Mo_4O_8 cubes and PO_4 tetrahedra. Of the six cube faces, four provide phosphate coordination sites. A phosphate always spans a pair of metal atoms not connected by a metal–metal bond, the remaining two phosphate oxygen atoms are ligated to a pair of metals from another cube. $Na_3[Mo_2O_4(PO_4)(HPO_4)]\cdot 2H_2O$[31] exemplifies the only polymeric compound built of covalently linked $\{Mo_2O_4\}^{2+}$ moieties; these are connected through phosphates, engaged in two distinct bridging roles, both different from the one described previously, into infinite sheets.

The closest relatives to **1** and **2** are the recently reported polymeric $(Me_4N)_2[Mo_2O_2As_2S_7]$ and $(Et_4N)_2[Mo_2O_2As_2Se_7]$.[35] The analogy becomes obvious by recognizing the alternating pattern of related dinuclear $\{Mo_2O_2(\mu\text{-}S)_2\}^{2+}$ or $\{Mo_2O_2(\mu\text{-}Se)_2\}^{2+}$ cores and bisbidentate $[As_2S_5]^{4-}$ or $[As_2Se_5]^{4-}$ ligands to form infinite, undulating chains. Similarly to the structural chemistry of $\{Mo_2O_4\}^{2+}$ core, the thio- and seleno-derivatized dimolybdenum(v) units find frequent occurrence in molecular compounds, but are only rarely incorporated into polymeric materials.

Synthetic considerations

The synthetic conditions leading to the formation of **1** and **2** merit comment. The polymeric phase **1** is obtained only when the oxalate to molybdate(v) ratio is slightly higher than the stoichiometric value of 0.5, while **2** requires a much greater excess of the oxalate. It is also noteworthy that **1** and **2**, both ionic compounds, crystallize from the relatively nonpolar media, *i.e.*, the reaction mixture contains mostly pyridine or 3-methylpyridine. In view of the relative ease with which the substitution of chlorides within the oxochloromolybdate(v) proceeds in the mixtures of pyridines and alcohols,[9] the retention of one coordinated chlorine per molybdenum was unexpected. Replacing the chloro coordinated starting material by the bromo analogue has a profound effect upon the reaction outcome, although the same oxalate *vs.* molybdate(v) ratio was used as for the preparation of **1**, a discrete dinuclear $[Mo_2O_4(\eta^2\text{-}C_2O_4)_2Py_2]^{2-}$ species was obtained.[36] Owing to the greater lability of bromo ligands compared to chloro, the substitution is complete and pyridine, which is present in huge excess, occupies the available coordination sites.

A very intriguing feature of **1** is the presence of the *N*-methylpyridinium cations which where generated inadvertently. *N*-Methylpyridinium salts result from a nucleophilic attack of pyridine on methyl halide formed from methanol and hydrogen halide. The latter reaction takes place only in a strongly acidic medium, which is not the case when working in pyridine. Moreover, halogenation of alcohols is known to take place more readily with tertiary and secondary alcohols, but not with methanol. Therefore molybdenum is assumed to play an important role in the transfer of a methyl group from the source to pyridine nitrogen. Preliminary reactions with other alcohols,[36] the synthesis of **2** also being an example, have shown that transfer of the alkyl group takes place at a detectable rate only when methanol is the source, while reactions with higher alcohols, a bulkier 2-propanol in the case of **2**, afford products which contain protonated pyridines *i.e.* 3-methylpyridinium cations in the case of **2**. Further efforts to elucidate the mechanisms governing the formation of *N*-methylpyridinium cations are in progress.

Vibrational spectra

The infrared spectra of **1** and **2** exhibit characteristic features of the bisbidentate oxalate:[37] $\nu_{as}(OCO)$ at 1670 and 1621 cm^{-1} for

1 and 1672 and 1629 cm^{-1} for **2**; ν_s(OCO) at 1353 and 1306 cm^{-1} for **1** and at 1353 and 1302 cm^{-1} for **2**; δ(OCO) at 803 cm^{-1} for **1** and at 799 cm^{-1} for **2**. The occurrence of two bands for the ν_{as}(OCO) and ν_s(OCO) vibrations has its origin in the asymmetrical coordination of the oxalate.[38]

The Mo=O vibrations can be easily identified as two sharp and strong absorptions at 965 and 943 cm^{-1} in the spectrum of **1**, and at 973 and 955 cm^{-1} in the spectrum of **2**.

A strong absorption at 316 cm^{-1} in the far IR spectrum of **1** and at 322 cm^{-1} in **2** is tentatively attributed to the Mo–Cl stretching vibration. Its position is comparable with those observed in molecular [$Mo_4O_8(OMe)_2Cl_2Py_4$] and [$Mo_4O_8(OMe)_2Cl_2$(4-MePy)$_4$].[9e]

Conclusions

The title compounds **1** and **2** are the second example where $\{Mo_2O_4\}^{2+}$ cores are incorporated into an extended array by means of bridging ligands. The oxalate is seen to occupy two out of three available coordination sites in each metal atom's environment. It is tempting to speculate whether further substitution by the oxalato ligands to produce higher-dimensional materials is also possible. In such instances, the oxalate would have to adopt another bridging role, presumably a less favourable bismonodentate coordination.[39]

Acknowledgements

We are grateful to the Slovenian Ministry of Education, Science and Sport for supporting this work through research grants PS-0508-0103 and SLO-US-2001/15. We also thank the same agency for funds to purchase the Nonius Kappa CCD diffractometer. The work at Syracuse University was supported by a grant from the National Science Foundation, CHE9987471.

References and notes

1 (*a*) See for example: M. J. Zaworotko, *Angew. Chem., Int. Ed.*, 2000, **39**, 3052; (*b*) B. J. S. Johnson, R. C. Schroden, C. Zhu, V. G. Young Jr. and A. Stein, *Inorg. Chem.*, 2002, **41**, 2213.

2 (*a*) A. Müller, S. Q. N. Shah, H. Bögge and M. Schmidtmann, *Nature*, 1999, **397**, 48; (*b*) A. Müller and P. Kögerler, *Coord. Chem. Rev.*, 1999, **182**, 3.

3 P. J. Hagrman, D. Hagrman and J. Zubieta, *Angew. Chem., Int. Ed.*, 1999, **38**, 2639 and references therein.

4 Exemplified by: [Mo_3O_9(2,2′-bipy)$_2$] (2,2′-bipy = 2,2′-bipyridine) in: (*a*) P. J. Zapf, R. C. Haushalter and J. Zubieta, *Chem. Mater.*, 1997, **9**, 2019; (*b*) [$MoO_3(Pyz)_{0.5}$] (Pyz = pyrazine) in: Y. Xu, J. Lu and N. K. Goh, *J. Mater. Chem.*, 1999, **9**, 1599.

5 Exemplified by: ($H_3N(CH_2)_2NH_3$)[Mo_3O_{10}] in: (*a*) M. I. Khan, Q. Chen and J. Zubieta, *Inorg. Chim. Acta*, 1993, **213**, 325; (*b*) ($H_3N(CH_2)_6NH_3$)[Mo_4O_{13}] in: Y. Xu, L.-H. An and L.-L. Koh, *Chem. Mater.*, 1996, **8**, 814; (*c*) (4,4′-bipyH_2)[Mo_7O_{22}]·H_2O in: P. J. Zapf, R. C. Haushalter and J. Zubieta, *Chem. Commun.*, 1997, 321.

6 (*a*) G. Luan, E. Wang, Z. Han and Y. Li, *Inorg. Chem. Commun.*, 2001, **4**, 541; (*b*) J. Niu, Q. Wu and J. Wang, *J. Chem. Soc., Dalton Trans.*, 2002, 2512.

7 (*a*) C. L. Hill (Guest editor), *Chem. Rev.*, 1998, **98**, 1; (*b*) *Polyoxometalates: From Platonic Solids to Anti-Retroviral Activity*, M. T. Pope and A. Müller, eds., Kluwer Academic Publishers, Dordrecht, The Netherlands, 1994.

8 H. K. Chae, W. G. Klemperer and T. A. Marquart, *Coord. Chem. Rev.*, 1993, **128**, 209.

9 Members of this series include a structural prototype of the $\{Mo_2O_4\}^{2+}$ unit, a dinuclear [$Mo_2O_4Cl_2$(R–Py)$_4$] (R–Py = alkyl-substituted pyridine), tetranuclear $(PyH)_2[Mo_4O_8(OR)_2(HOR)_2X_4]$, [$Mo_4O_8(OR)_2X_2Py_4$] (R = Me, Et; X = Cl, Br), [$Mo_4O_8(OMe)_4$(4-MePy)$_4$], pentanuclear [$Mo^V_4Mo^{VI}O_{11}(OMe)_4Py_4$], hexanuclear [$Mo_6O_{12}(OMe)_6Py_4$], two structural isomers of octanuclear [$Mo_8O_{16}(OMe)_8$(R–Py)$_4$], decanuclear [$Mo^V_8Mo^{VI}_2O_{26}$(R–Py)$_8$] and dodecanuclear [$Mo_{12}O_{28}(OMe)_2X_2$(R–Py)$_8$]. For a more detailed account see: (*a*) B. Modec, J. V. Brenčič and I. Leban, *Inorg. Chem. Commun.*, 1998, **1**, 161; (*b*) B. Modec, J. V. Brenčič, R. Rotar, L. Golič and K. Prout, *Acta Crystallogr., Sect. C*, 1998, **54**, 1573; (*c*) B. Modec, J. V. Brenčič and L. Golič, *Polyhedron*, 2000, **19**, 1219; (*d*) B. Modec, J. V. Brenčič, L. Golič and L. M. Daniels, *Polyhedron*, 2000, **19**, 1407; (*e*) B. Modec, J. V. Brenčič, L. Golič and G. Giester, *Inorg. Chim. Acta*, 2000, **307**, 32; (*f*) B. Modec, J. V. Brenčič, J. Zubieta and P. J. Hagrman, *Inorg. Chem. Commun.*, 2001, **4**, 537; (*g*) B. Modec, J. V. Brenčič, R. C. Finn, R. S. Rarig and J. Zubieta, *Inorg. Chim. Acta*, 2001, **322**, 113; (*h*) B. Modec, J. V. Brenčič and J. Zubieta, *J. Chem. Soc., Dalton Trans.*, 2002, 1500; (*i*) B. Modec and J. V. Brenčič, *J. Cluster Sci.*, 2002, **13**, 279.

10 R. C. Haushalter and L. A. Mundi, *Chem. Mater.*, 1992, **4**, 31.

11 G. R. Hanson, A. A. Brunette, A. C. McDonell, K. S. Murray and A. G. Wedd, *J. Am. Chem. Soc.*, 1981, **103**, 1953.

12 SMART and SAINT, Siemens Analytical X-ray Instruments Inc., Madison, WI, 1990.

13 G. M. Sheldrick, SADABS, A Program for Absorption Correction with the Siemens SMART Area-Detector System, University of Göttingen, 1996.

14 Z. Otwinowski and W. Minor, *Methods Enzymol.*, 1997, **276**, 307.

15 G. M. Sheldrick, SHELXS 97 and SHELXL 97, Programs for Crystal Structure Solution and Refinement, University of Göttingen, 1997.

16 SHELXTL version 5.03, Software Package for Crystal Structure Determination, Siemens Analytical X-ray Instrument Division, Madison, WI, 1994.

17 A. Bernalte, F. J. G. Barros, I. Cavaco, J. Costa Pessoa, R. D. Gillard, F. J. Higes and I. Tomaz, *Polyhedron*, 1998, **17**, 3269.

18 (*a*) O. Castillo, A. Luque, P. Roman, F. Lloret and M. Julve, *Inorg. Chem.*, 2001, **40**, 5526; (*b*) R. Vaidhyanathan, S. Natarajan and C. N. R. Rao, *J. Chem. Soc., Dalton Trans.*, 2001, 699; (*c*) J. Salta, C. J. O'Connor, S. Liu and J. Zubieta, *Inorg. Chim. Acta*, 1996, **250**, 303.

19 B. Kamenar, B. Kaitner and N. Strukan, *Croat. Chem. Acta*, 1991, **64**, 329.

20 H.-F. Lang, P. E. Fanwick and R. A. Walton, *Inorg. Chim. Acta*, 2002, **328**, 232.

21 T. Shibahara, H. Kuroya, K. Matsumoto and S. Ooi, *Inorg. Chim. Acta*, 1981, **54**, L75.

22 A. Johansson, M. Roman, G. A. Seisenbaeva, L. Kloo, Z. Szabo and V. G. Kessler, *J. Chem. Soc., Dalton Trans.*, 2000, 387.

23 M. J. Manos, A. D. Keramidas, J. D. Woollins, A. M. Z. Slawin and T. A. Kabanos, *J. Chem. Soc., Dalton Trans.*, 2001, 3419.

24 F. A. Cotton and S. M. Morehouse, *Inorg. Chem.*, 1965, **10**, 1377.

25 Q. Chen, S. Liu and J. Zubieta, *Angew. Chem., Int. Ed. Engl.*, 1988, **27**, 1724.

26 Q. Chen, S. Liu and J. Zubieta, *Inorg. Chem.*, 1989, **28**, 4433.

27 T. Shibahara, S. Ooi and H. Kuroya, *Bull. Chem. Soc. Jpn.*, 1982, **55**, 3742.

28 (*a*) A. Dolbecq, B. Salignac, E. Cadot and F. Secheresse, *Bull. Pol. Acad. Sci.*, 1998, **46**, 237; (*b*) F. Secheresse, E. Cadot and A. Dolbecq, *J. Solid State Chem.*, 2000, **152**, 78.

29 M. I. Khan, Y.-D. Chang, Q. Chen, J. Salta, Y.-S. Lee, C. J. O'Connor and J. Zubieta, *Inorg. Chem.*, 1994, **33**, 6340.

30 W. S. McDonald, *Acta Crystallogr., Sect. B*, 1978, **34**, 2850.

31 L. A. Mundi and R. C. Haushalter, *Inorg. Chem.*, 1990, **29**, 2879.

32 $(Et_4N)_2[Mo_4O_8(PO_4)_{2/2}(H_{1.5}PO_4)_2]\cdot 2H_2O$ in: L. A. Mundi and R. C. Haushalter, *J. Am. Chem. Soc.*, 1991, **113**, 6340.

33 $(N(C_3H_7)_4)(NH_4)[Mo_4O_8(PO_4)_2]$ in: E. W. Corcoran Jr., *Inorg. Chem.*, 1990, **29**, 157.

34 $(Me_4N)_{1.3}(H_3O)_{0.7}[Mo_4O_8(PO_4)_2]\cdot 2H_2O$ in: R. C. Haushalter, K. G. Strohmaier and F. W. Lai, *Science*, 1989, **246**, 1289.

35 J.-H. Chou, J. A. Hanko and M. G. Kanatzidis, *Inorg. Chem.*, 1997, **36**, 4.

36 B. Modec, J. V. Brenčič and D. Dolenc, unpublished work.

37 (*a*) N. F. Curtis, *J. Chem. Soc. A*, 1968, 1584; (*b*) P. Roman, C. Guzman-Miralles, A. Luque, J. I. Beitia, J. Cano, F. Lloret, M. Julve and S. Alvarez, *Inorg. Chem.*, 1996, **35**, 3741.

38 I. Castro, J. Faus, M. Julve and A. Gleizes, *J. Chem. Soc., Dalton Trans.*, 1991, 1937.

39 O. Castillo, A. Luque, J. Sertucha, P. Roman and F. Lloret, *Inorg. Chem.*, 2000, **39**, 6142.